

## Testing a Fine-Needle Optical Probe for Recording Changes in the Fluorescence of Coenzymes of Cellular Respiration

K. Yu. Kandurova<sup>a,\*</sup>, E. V. Potapova<sup>a</sup>, E. A. Zherebtsov<sup>a,b</sup>, V. V. Dremin<sup>a,b</sup>, E. S. Seryogina<sup>a</sup>,  
A. Yu. Vinokurov<sup>c</sup>, A. V. Mamoshin<sup>a,d</sup>, A. V. Borsukov<sup>e</sup>, Yu. V. Ivanov<sup>f,g</sup>, and A. V. Dunaev<sup>a</sup>

<sup>a</sup>Research and Development Center of Biomedical Photonics, Orel State University, Orel, 302026 Russia

<sup>b</sup>University of Oulu, Optoelectronics and Measurement Techniques Unit, Oulu, 90570 Finland

<sup>c</sup>Department of Industrial Chemistry and Biotechnology, Orel State University, Orel, 302026 Russia

<sup>d</sup>Orel Regional Clinical Hospital, Orel, 302028 Russia

<sup>e</sup>Problem Research Laboratory “Diagnostic Researches and Mini-invasive Technologies,”  
Smolensk State Medical University, Smolensk, 214006 Russia

<sup>f</sup>Federal Scientific and Clinical Center for Specialized Medical Service and Medical Technologies,  
Federal Biomedical Agency of Russia, Moscow, 115682 Russia

<sup>g</sup>Central Research Institute of Tuberculosis, Moscow, 107564 Russia

\*e-mail: kandkseniya@gmail.com

Received December 10, 2019; revised January 31, 2020; accepted February 28, 2020

**Abstract**—A device for optical biopsy with a fluorescence spectroscopy channel and a fine-needle optical probe for use in fine-needle aspiration biopsy of liver tumors is described. To test the developed device, experimental measurements of the fluorescence of internal organs of a laboratory rat were carried out in vivo while exposing the tissue surface to mitochondrial uncoupling to induce changes in cell respiration. The results of the model experiment showed the ability of the developed channel to detect changes in fluorescence due to changes in the processes of oxidative phosphorylation of mitochondria.

**Keywords:** optical biopsy, fluorescence spectroscopy, mitochondrial uncouplers, NADH, FAD

**DOI:** 10.1134/S0030400X20060089

### INTRODUCTION

According to the World Health Organization’s statistics, cancer is the second leading cause of death in the world [1]. Liver cancer is the type of oncopathology that is difficult to diagnose. Primary liver cancer is the sixth most prevalent in the world and the fourth most fatal among other types of malignant neoplasms [2, 3]. The number of registered cases of this disease tends to increase [4, 5]. Metastases in the liver most often occur due to malignant neoplasms in other organs [6]. The possibility of earlier diagnosis is among the factors that improve prognosis in patients with liver tumors.

Despite the current technical and methodological level of medicine, the diagnosis of liver cancer still meets certain difficulties. Histological and cytological studies of tissue and cell samples are the “gold standard” of preoperative diagnosis of malignant tumors [7]. For these studies, fine-needle aspiration biopsy (FNAB) is performed [8, 9], in which a tissue sample is collected from several areas of the pathological site under investigation using a thin needle with a normal or cutting edge under the control of visualization

methods such as ultrasound, computer tomography, or magnetic resonance imaging. The advantages of this procedure include minimal invasiveness, low likelihood of complications, high accuracy, and cost efficiency [10]. The tissue obtained during FNAB is sent for routine histopathological and cytological studies. The surgeon receives the results 5–10 days after the procedure, while obtaining information about the state of the tissues of the affected organ during this period is of interest for selecting tactics for further treatment. Another problem of the method is the probability of collecting noninformative material, for example, due to physiological displacement of organs, manipulations preceding FNAB, involuntary patient movements, or insufficient visualization of the tumor site due to its small size and heterogeneity. The above factors lead to the fact that even experienced surgeons collect up to 15–29% of inadequate samples [11–13]. A false negative result leads to the need for a second procedure, which may be associated with a risk of complications for the patient and increases the duration of treatment. To improve the treatment of patients with liver malignant neoplasms, the urgent task is to

develop and introduce new diagnostic methods that allow obtaining real-time information.

Optical biopsy is one of the rapidly developing fields of application of biomedical optics for solving surgical problems [14]. It combines the advantages of conventional biopsy and compensates its main drawback, that is, the need to remove a tissue sample and spend significant time to analyze it. The optical biopsy includes several spectroscopic and visualization methods [15, 16], which yield additional diagnostic *in vivo* information about various parameters of the morphology and metabolism of biological tissues [17, 18]. In optical fine-needle aspiration biopsy using small outer-diameter needles (14–22 G or 0.7–2.1 mm), the development of fine-needle optical probes for implementing various spectroscopic diagnostic methods is the most common field of preclinical studies [19–24].

Among optical diagnostic methods, fluorescence spectroscopy (FS) has found widespread use for studying the metabolic activity of healthy and pathologically altered tissue cells (inflamed, malignant, etc.) in some medical fields [25, 26]. This method is based on the excitation of fluorescence of endogenous or exogenous fluorophores in biological tissue by monochromatic radiation of the near ultraviolet (UV) or visible ranges and further recording of the resulting spectrum for analysis and comparison. In several studies, fluorescence spectroscopy is used as the main diagnostic method or as part of multimodal devices having fine-needle fiber optic probes for the diagnosis of tumor formations of the lungs [27, 28] and mammary glands [29, 30].

Many forms of coenzymes of nicotinamide adenine dinucleotide (NAD) and flavin adenine dinucleotide (FAD), contained in the cytosol and mitochondria of cells, have pronounced endogenous fluorescence spectra, changes in the intensity of which can be recorded *in vivo*. This phenomenon is the base of studies of tissue metabolic activity [31–34]. These coenzymes are an integral part of cellular metabolism reactions, acting as electron donors and acceptors for the synthesis of adenosine triphosphate (ATP) molecules, which supply energy for other numerous biochemical reactions [35]. Both coenzymes undergo oxidation and reduction reactions, while of all forms, reduced NAD (NADH) and oxidized FAD make the largest contribution to the formation of tissue fluorescence spectra. Previous clinical studies have shown that changes in the fluorescence intensities of NADH and FAD in tissues are associated with the occurrence of pathological processes in them, including the development of oncological processes [36]. The tissue fluorescence spectrum recorded by the spectrometer is a consequence of the addition of fluorescence signals not only of NADH and FAD but also of other endogenous fluorophores, like collagen, elastin, porphyrins, lipofuscin, bilirubin, etc. Fluorescence of these substances is also excited by light with short wavelengths

close to the wavelengths of excitation of redox coenzymes. For this reason, we should take into account the contribution of NADH and FAD to the total recorded fluorescence signal to interpret the differences observed between healthy and pathologically altered tissues correctly.

The development of the FS channel for optical biopsy of malignant neoplasms requires reliable and reproducible measurements of the spectral characteristics of normal and pathological tissues in the test area. For the further introduction of the technology into clinical practice, it is necessary to conduct studies aimed at assessing the sensitivity of optical biopsy devices to changes in the fluorescence signal, reflecting metabolic activity in cell mitochondria, and developing methods for adjusting the recorded spectrum for a more accurate interpretation of the data. A common way to test fluorescence diagnostic devices is to use specially developed test objects (phantoms). Such phantoms possess optical properties close to biological tissues; they are made to simulate spectral characteristics determined by the concentration of various fluorophores [37–39]. Another direction is *in vitro* and *in vivo* studies evaluating the effect of factors that can cause changes in metabolic activity in tissues. One of these factors is the use of a wide range of mitochondrial inhibitors and uncouplers that directly affect mitochondrial function. Their action manifests itself in an abnormal increase or decrease in the accumulation of coenzymes NADH and FAD during biochemical reactions and, therefore, gives a response when measuring fluorescence intensity [40–42]. However, most protocols for such studies have been developed and are used for measurements in cell cultures [43–47]; few works are devoted to studies adapting this approach to the whole organs of model animals [32, 48].

The goal of this work was to study the sensitivity of the measuring channel of an FS device for fine-needle optical biopsy to the concentration of the main target endogenous fluorophores associated with cellular metabolism, to demonstrate the capability of the developed device of assessing the state of biological tissues *in situ* and *in vivo*.

## EXPERIMENTAL

A model experiment was carried out using a device specially designed for optical biopsy [49], which contains two measuring channels: FS and diffuse reflectance spectroscopy (DRS). In the FS channel, NADH and FAD autofluorescence was excited by LED radiation at a wavelength of 365 nm and a laser diode radiation with a wavelength of 450 nm [50]. The output power of the sources used was not more than 1.5 and 3.5 mW, respectively, which ensures compliance with safety requirements for effective illumination of tissues [51, 52] and lowers the effect of photobleaching of coenzymes. To attenuate the backscattered radiation

of the sources, FGL400 and FGL495 filters (Thorlabs, United States) with cut-off wavelengths of 400 and 495 nm were used with the sources, respectively. To record the fluorescence spectra in the range of 350–1000 nm, we used a FLAME-T-VIS-NIR-ES small-size CCD spectrometer (Ocean Optics, United States).

The DRS channel is necessary to compensate for the effect of tissue blood supply on the fluorescence signal; it can also be used to obtain additional information about the morphological structure of tissues. The channel contains an HL-2000-FHSA broadband tungsten-halogen radiation source (Ocean Optics, United States) with a range of 360–2400 nm. The control of the device and processing of the obtained data were carried out using specially developed software in the MATLAB environment.

We used a specially developed fine-needle optical probe with an outer diameter of 1 mm to transmit radiation from sources and collect secondary optical radiation from biological tissue. The probe can be introduced into the studied area through a fine needle with an outer diameter of 17.5 G (Fig. 1). The probe contains ten optical fibers: a central fiber with a diameter of 200  $\mu\text{m}$  is used to collect radiation and transmit it to the spectrometer, and nine fibers with a diameter of 100  $\mu\text{m}$  (three fibers for each source) serve to illuminate the study area uniformly during measurements. The end of the fiber probe has a bevel of 20° to ensure tight contact with the tissues. The value of the numerical aperture of the optical fibers in the probe is 0.22.

We used an oxidative phosphorylation uncoupler (protonophore), namely, carbonyl cyanide *m*-chlorophenyl hydrazone (CCCP), to simulate rapid changes in the metabolic activity of tissues. The CCCP compound is an inhibitor of oxidative phosphorylation, increasing the permeability of the mitochondrial membrane, thereby violating the proton gradient [53]. The application of CCCP to the surface of the tissue decreases the concentration of NADH in the cells; the content of FAD, on the contrary, increases. Disruption of proton transfer along the electron transport chain leads to the insufficient synthesis of ATP molecules, which causes the gradual destruction of cells and the death of the body [54].

To obtain the initial CCCP solution from a concentrate (Sigma-Aldrich, United States), we selected dimethyl sulfoxide (DMSO) as a solvent [46]. This substance is widely used in chemical research as an organosulfur solvent for other substances. In biophotonics, DMSO is used for optical bleaching of biological tissues [55], its antireflection properties are retained after a long time after exposure [56]. Another feature of DMSO, essential for this work, is its ability not only to penetrate biological tissues but also to transfer other chemical compounds into them [57, 58], which can be used to observe the effect of using a CCCP solution more clearly.

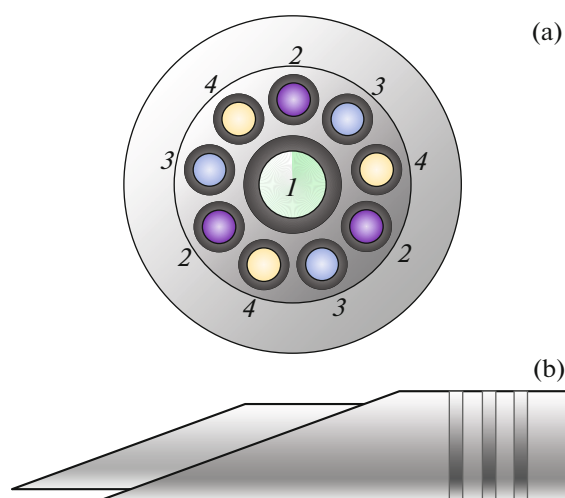


**Fig. 1.** (a) Arrangement of optical fibers in a fine-needle optical probe of an optical biopsy device: (1) fiber to the spectrometer, (2) fiber from a 365-nm source, (3) fiber from a 450-nm source, and (4) fiber from a broadband source. (b) Location of the optical probe in the standard needle 17.5 G.

To select the optimal values of the reliable signal of tissue fluorescence, depending on the type of tissue itself and the characteristics of the developed FS channel, various concentrations of CCCP solution were tested during the experiment. We used a stock CCCP solution at a concentration of 1 mM and dilute solutions at a concentration of 0.1 and 0.01 mM, obtained by dilution of the stock solution with a sodium phosphate buffer solution (PBS). The DMSO solution at the initial concentration of 100% and concentrations of 10 and 1% after dilution in PBS was used for a blank experiment without uncoupler.

A clinically healthy male Wistar rat (3 months old) was used in the study. The rat was anesthetized with Zoletil 100 (Vibrac, France) in a standard dose and fixed on a special platform. At the first stage of the experiment, the measurements were carried out after applying DMSO and CCCP solutions with a micropipette on the previously prepared abdominal skin. At the second stage, a laparotomy was performed, followed by the application of solutions on the surface of the liver, heart, and skeletal muscles of the back rat limbs. The fluorescence spectra were recorded with an interval of 1 s. A schematic representation of the experiment is shown in Fig. 2.

After recording the fluorescence spectra, the maximum values of the fluorescence intensity in the ranges of 480–530 nm (for the radiation source of 365 nm) and 500–550 nm (for the radiation source of 450 nm) were selected to analyze the dynamics of the signal over time. We estimated the relative change in the fluorescence intensity during the experiment by calculating the ratio of the fluorescence intensity in the  $N$ th second of the  $IF_N$  experiment to the fluores-

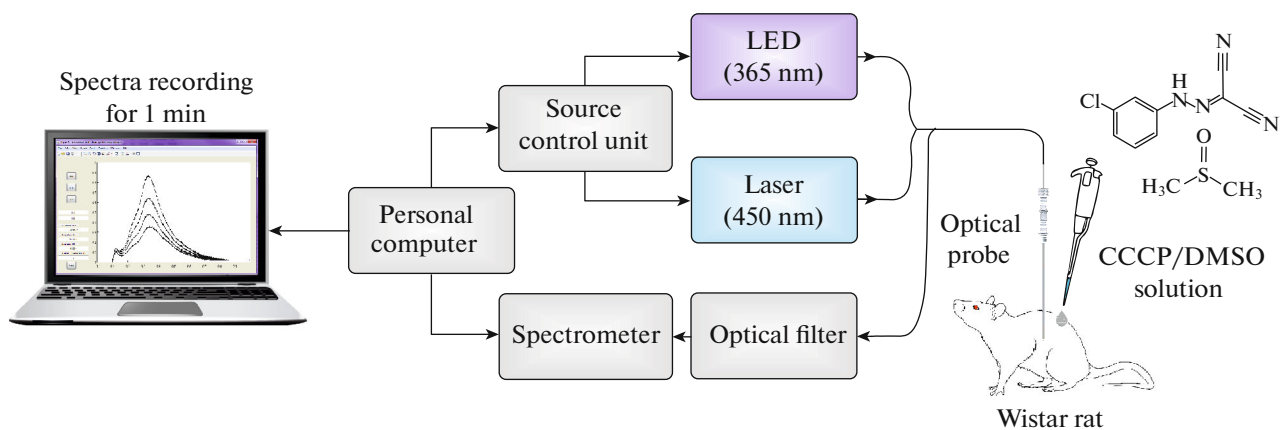


**Fig. 2.** Schematic diagram of an experimental setup using a fluorescence spectroscopy channel of a device for conducting fine-needle optical biopsy.

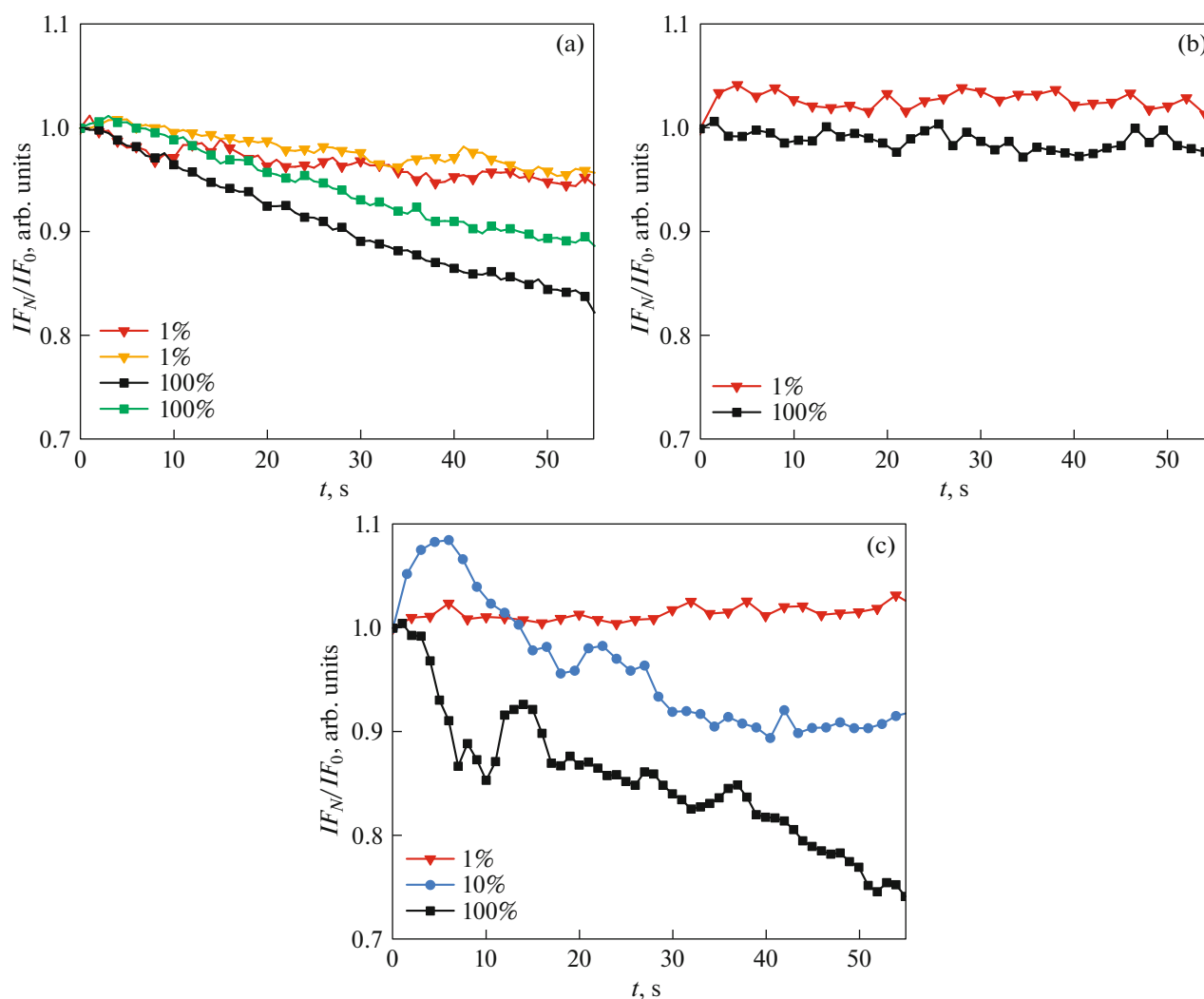


**Fig. 3.** Changes in the maximum fluorescence intensity in the ranges of 480–530 nm for a radiation source of 365 nm after applying various concentrations of DMSO; areas of study: (a) skin, (b) muscle, and (c) liver.

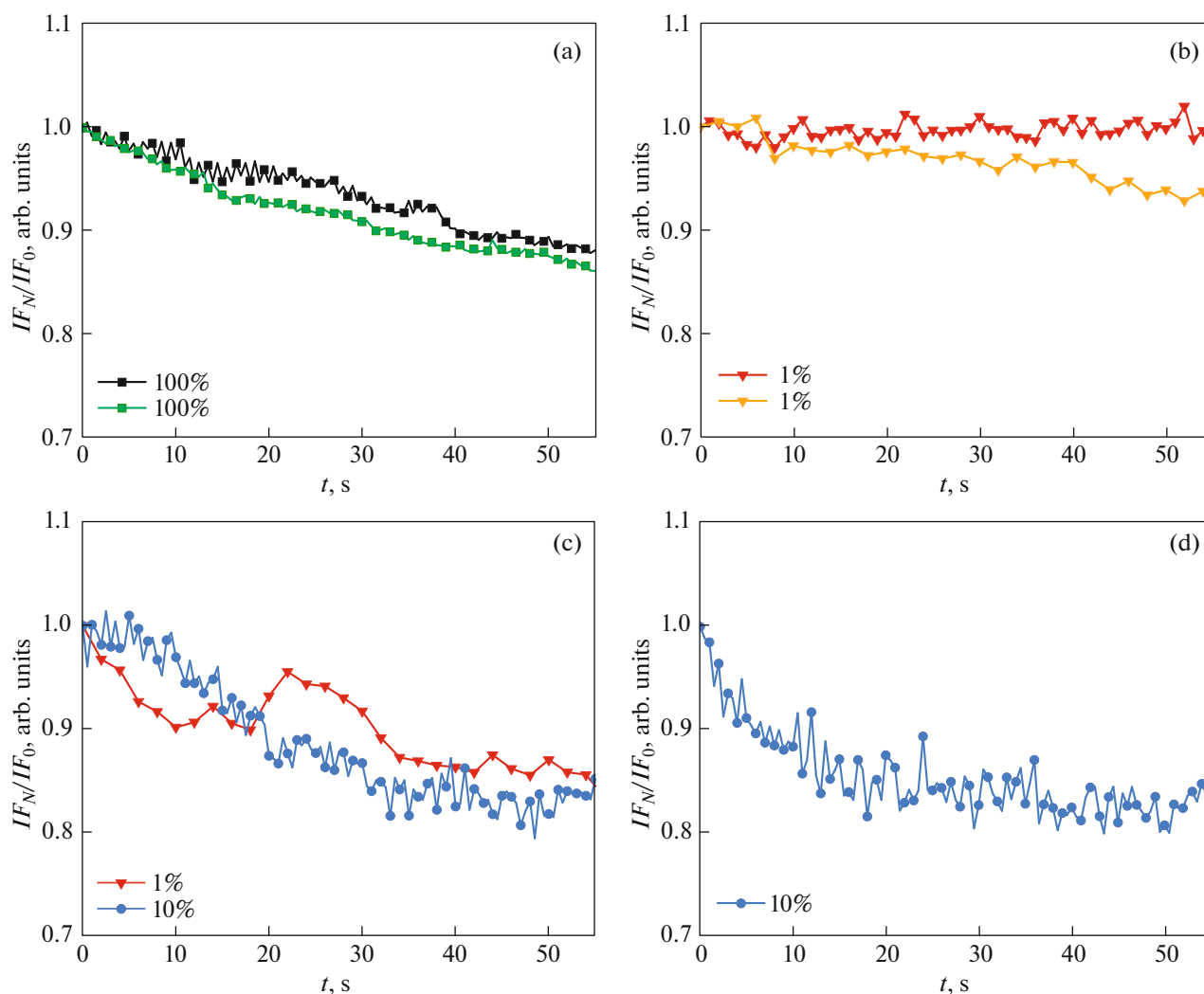


**Fig. 4.** Changes in the maximum fluorescence intensity in the ranges of 500–550 nm for a radiation source of 450 nm after applying various concentrations of DMSO; areas of study: (a) skin, (b) muscle, (c) liver, and (d) heart.

cence intensity recorded at the beginning of  $IF_0$  measurements. Based on the obtained relations, the curves of changes in the maximum fluorescence intensities with time were constructed.

## RESULTS AND DISCUSSION

The power of the radiation sources was selected regarding the measures to lower the effect of photobleaching. At the beginning of each measurement, before applying the DMSO and CCCP solutions, fluorescence spectra were recorded under continuous illumination of the tissue to take into account the presence of this effect. Slight photobleaching of tissues was observed in some cases; on average, this effect was more pronounced for a radiation source of 450 nm. If photobleaching was not expressed, solutions of substances were applied, and an array of spectra was recorded. Part of the signals at various concentrations

of substances acting on the tissues of organs were found to be unsatisfactory due to the low signal-to-noise ratio and were not taken into account when analyzing the data.

The dynamics of changes in the maximum fluorescence intensity under exposure to DMSO solutions (Figs. 3 and 4) show that the fluorescence spectra of the skin and muscle tissue have satisfactory reproducibility. The fluorescence of muscle tissue remained relatively stable (the signal drop was no more than 10%) under the effect of a DMSO solution with different concentrations upon excitation by radiation of both 365 and 450 nm. The signal drop at the skin was 10% or higher in the case of tissue interaction with a higher (100%) concentration of DMSO. The fluorescence intensity in the tissues of the liver and heart decreased more significantly; in particular, in the liver, the decrease reached more than 25% (when excited by

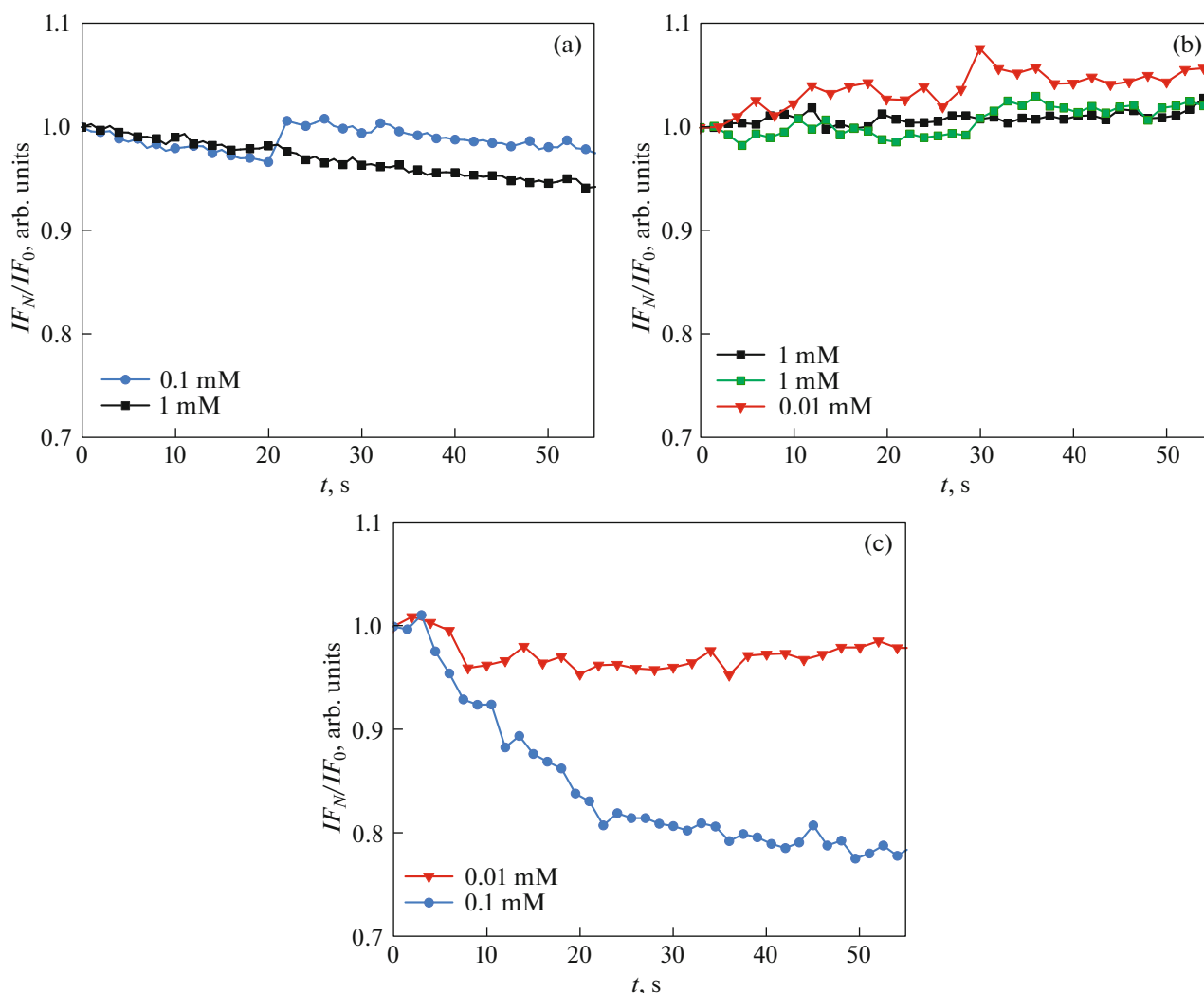


**Fig. 5.** Changes in the maximum fluorescence intensity in the ranges of 480–530 nm for a radiation source of 365 nm after applying various concentrations of CCCP; areas of study: (a) skin, (b) muscle, and (c) liver.

radiation of 450 nm) even at low concentrations of the active agent.

Upon excitation at 365 nm, the signal drop was significant only when the liver tissue was exposed to a pure solution of DMSO. We took measures to record data without the effect of photobleaching; therefore, we assumed that this might be caused by the toxic effect of DMSO, which may manifest itself in changes in the structure of the cell membrane at certain concentrations. It is believed that *in vivo* studies, DMSO has no toxic effect at concentrations up to 10% [59, 60], but at higher concentrations, this substance exhibits the properties of a mitochondrial respiration inhibitor and leads to apoptosis of cells [61, 62]. Also, data are published about the mechanisms of the toxic effects of DMSO when using concentrations of 2–4% [63].

As with measurements with DMSO solutions, we noted that skin and muscle tissues showed a lower

response to CCCP, regardless of the substance concentration, in contrast to liver and heart tissues. Perhaps this is because CCCP and DMSO had a multidirectional effect on the fluorescence signal and partially compensated each other.

After exposure of liver tissue to a CCCP solution with a concentration of 0.1 mM, the fluorescence induced by 365-nm radiation decreased as much as upon exposure to a 100% DMSO solution (Fig. 5c), while the main decrease the fluorescence intensity occurred for the first 20 s. The violation of oxidative phosphorylation due to the uncoupling of proton transition leads to increased electron consumption, which results in more active oxidation of the electron donor NADH to NAD. Since NAD does not have the same pronounced fluorescence spectrum as NADH, a decrease in the concentration of the reduced form of coenzyme in cells becomes noticeable by a character-

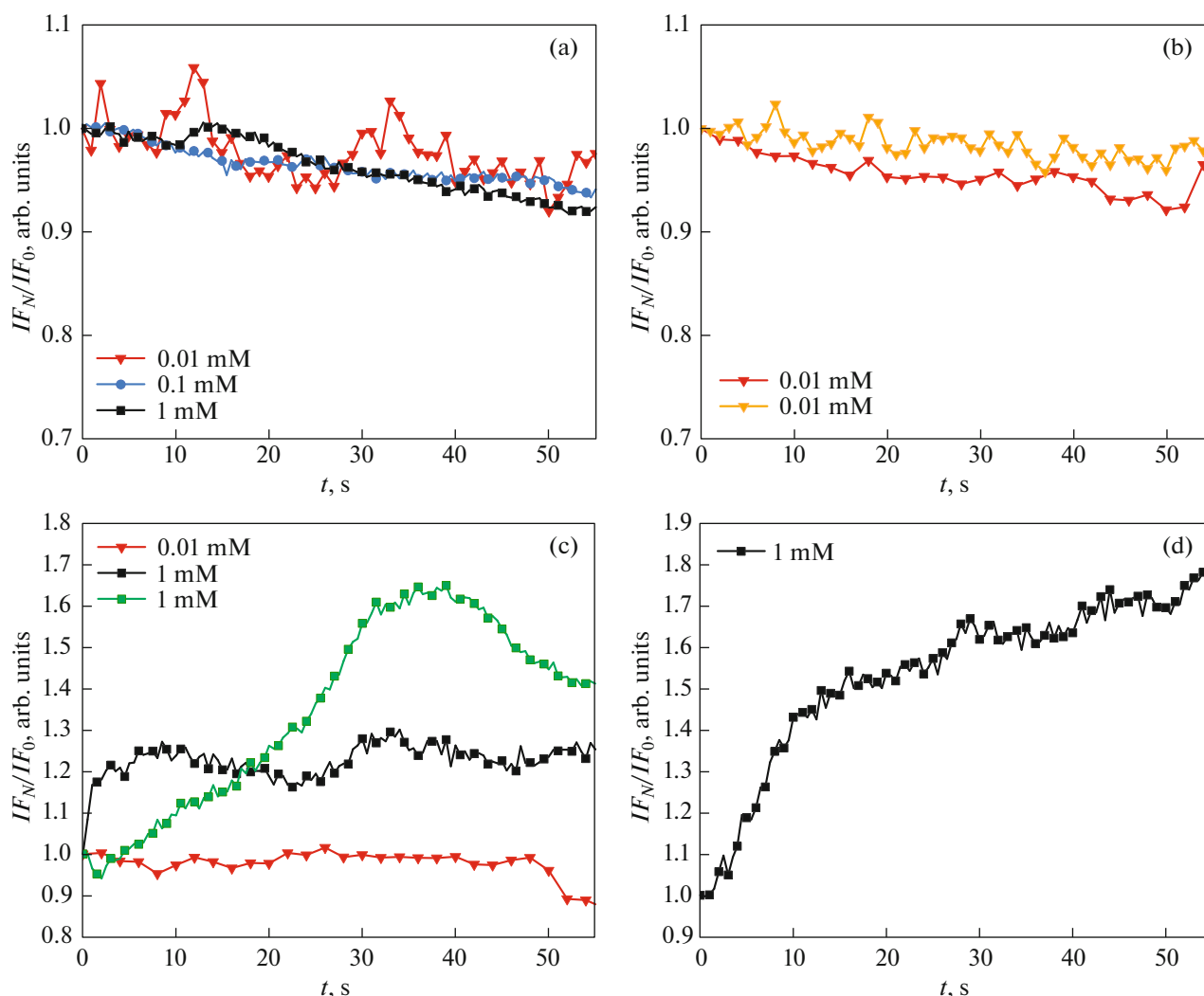


**Fig. 6.** Changes in the maximum fluorescence intensity in the ranges of 500–550 nm for a radiation source of 450 nm after applying various concentrations of CCCP; areas of study: (a) skin, (b) muscle, (c) liver, and (d) heart.

istic decrease in the maximum fluorescence intensity over time [46].

Upon excitation of the tissues of the heart and liver with 450-nm radiation, the application of a 1 mM CCCP solution caused a significant increase in fluorescence (Fig. 6). The dynamics of the signal growth in time may be explained as follows. As CCCP causes increased mitochondrial activity by stimulation of oxidative phosphorylation reactions and increases electron consumption, an increasing number of reduced  $\text{FADH}_2$  molecules are oxidized to FAD, which leads to an increase in fluorescence intensity [64].

The results of experimental studies showed that the skin and skeleton parietal muscles of the rat hind paw were less susceptible to the described chemical exposures, while the internal organs (liver, heart) were more sensitive and underwent both the expected effect of uncoupling of oxidative phosphorylation upon exposure to CCCP and the toxic effect of the DMSO

solvent. The use of different concentrations of solutions did not cause differences in the rate or magnitude of changes in the fluorescence intensity of the skin and muscles, while the use of high concentrations of solutions for the liver and heart tissues made it possible to achieve a more pronounced and faster manifestation of changes in fluorescence intensity due to the effect on the metabolic activity of cells in tissues *in vivo*.

## CONCLUSIONS

The use of a wide variety of optical biopsy methods currently seems to be a promising direction for the introduction of into clinical practice, since they allow obtaining additional diagnostic information about the metabolic state and morphological structure of biological tissues in real time, which can be essential in the treatment of oncological diseases. Fluorescence spectroscopy is one of the promising methods for an

initial diagnostic assessment of liver neoplasms already in the process of FNAB, which can be introduced even in conventional biopsy needles. In this work, we tested *in vivo* the sensitivity of the FS channel of a device developed earlier for optical biopsy during the FNAB procedure to metabolic changes in the mitochondria of cells. This is essential for evaluating carcinogenesis processes in biological tissues, including the liver, one of the distinguishing features of which is metabolic disorders caused by active tumor growth.

The development of protocols and *in vivo* studies of the effect of factors that can cause changes in the processes of oxidative phosphorylation of mitochondria can form the basis for a more accurate interpretation of FS data. The results obtained in this work show the possibility of adapting the *in vitro* methodology for analyzing cell metabolism to such *in vivo* measurements in organ tissues. However, further studies are needed aiming at experimental selection of the optimal concentrations of CCCP and DMSO, taking into account the results obtained in this work, including conclusions about the toxicity of DMSO on tissues *in vivo*. The results presented in this work demonstrated a more pronounced effect for the fluorescence spectra contributed mainly by the change in the FAD concentration; therefore, it is of interest to observe a similar effect caused by changes in NADH. We suggest the use of other mitochondrial inhibitors and uncouplers in further studies. For these purposes, a rotenone inhibitor can be used blocking the electron transfer through complex I, an excess of which is reflected in the rapid increase in the NADH concentration without significant changes in the FAD concentration [65].

The results showed the capability of the FS channel of an optical biopsy device of detecting fluorescence changes caused by metabolic changes in tissues, which confirms the validity of using the device for FNAB in clinical practice, including in the diagnosis of liver tumors.

#### FUNDING

This work was supported by the Russian Science Foundation, project no. 18-15-00201.

#### COMPLIANCE WITH ETHICAL STANDARDS

##### *Statement on the Welfare of Animals*

The studies were carried out under the Principles of Good Laboratory Practice (GLP) set by the Organization for Economic Cooperation and Development (OECD) and were approved by the ethics committee of Orel State University (minutes of the meeting no. 12 of September 6, 2018).

##### *Conflict of Interest*

The authors declare that they have no conflict of interest.

#### REFERENCES

1. *The Cancer Atlas*, 3rd ed. (Int. Agency Research on Cancer, 2019). <https://canceratlas.cancer.org>.
2. J. Ferlay, I. Soerjomataram, M. Ervik, R. Dikshit, S. Eser, C. Mathers, M. Rebelo, D. M. Parkin, D. Forman, and F. Bray, *Cancer Incidence, Mortality and Prevalence Worldwide in 2012 v1.0* (2013).
3. Liver Cancer Fact Sheet. Global Cancer Observatory, 2018. <http://gco.iarc.fr/today/fact-sheets-cancers>.
4. T. Clark, S. Maximin, J. Meier, S. Pokharel, and P. Bhargava, *Curr. Probl. Diagn. Radiol.* **44**, 479 (2015). <https://doi.org/10.1067/j.cpradiol.2015.04.004>
5. P. C. Valery, M. Laversanne, P. J. Clark, J. L. Petrick, K. A. McGlynn, and F. Bray, *Hepatology* **67**, 600 (2018). <https://doi.org/10.1002/hep.29498>
6. D. A. Mahvi and D. M. Mahvi, *Abeloff's Clinical Oncology* (2020), p. 846.
7. H. Gharib, E. Papini, R. Paschke, D. S. Duick, R. Valcavi, L. Hegedus, and P. Vitti, *Endocrine Practice* **16** (Suppl. 1), 1 (2010). <https://doi.org/10.4158/EP.16.3.468>
8. M. B. Pitman, *Clin. Lab. Med.* **18**, 483 (1998). [https://doi.org/10.1016/S0272-2712\(18\)30160-4](https://doi.org/10.1016/S0272-2712(18)30160-4)
9. A. Wee, *Patholog. Res. Int.* **2011**, 587936 (2011). <https://doi.org/10.4061/2011/587936>
10. D. C. Chhieng, *World J. Surg. Oncol.* **2**, 5 (2004). <https://doi.org/10.1186/1477-7819-2-5>
11. S. H. Choi, K. H. Han, J. H. Yoon, H. J. Moon, E. J. Son, J. H. Youk, E. Kim, and J. Y. Kwak, *Clin. Endocrinol. (Oxford)* **74**, 776 (2011). <https://doi.org/10.1111/j.1365-2265.2011.04011.x>
12. G. S. Gomez-Macias, R. Garza-Guajardo, J. Segura-Luna, and O. Barboza-Quintana, *Cytojournal* **6**, 9 (2009). <https://doi.org/10.4103/1742-6413.52831>
13. A. Kalogeraki, G. Z. Papadakis, D. Tamiolakis, I. Karvela-Kalogeraki, M. Karvelas-Kalogerakis, J. Segredakis, and E. Moustou, *Rom. J. Int. Med.* **53**, 209 (2015). <https://doi.org/10.1515/rjim-2015-0028>
14. R. Alfano and Y. Pu, *Lasers for Medical Applications* (Woodhead, 2013), p. 325.
15. K. Y. Kandurova, V. V. Dremin, E. A. Zhrebtsov, A. L. Alyanov, A. V. Mamoshin, E. V. Potapova, A. V. Dunaev, V. F. Muradyan, V. V. Sidorov, and A. I. Krupatkin, *Region. Blood Circul. Microcircul.* **17**, 71 (2018). <https://doi.org/10.24884/1682-6655-2018-17-3-71-79>
16. T. D. Wang and J. van Dam, *Clin. Gastroenterol. Hepatol.* **2**, 744 (2004). [https://doi.org/10.1016/S1542-3565\(04\)00345-3](https://doi.org/10.1016/S1542-3565(04)00345-3)
17. V. V. Tuchin, *Handbook of Optical Biomedical Diagnostics* (Fizmatlit, Moscow, 2007; SPIE Press, 2002), Vol. 1.
18. G. T. Kennedy, O. T. Okusanya, J. J. Keating, D. F. Heitjan, C. Deshpande, L. A. Litzky, S. M. Albelda, J. A. Drebin, S. Nie, P. S. Low, and S. Singhal, *Ann. Surg.* **262**, 602 (2015). <https://doi.org/10.1097/SLA.0000000000001452>



19. L. Alchab, G. Dupuis, C. Balleyguier, M. Mathieu, M. Fontaine-Aupart, and R. Farcy, *J. Biophoton.* **3**, 373 (2010).  
<https://doi.org/10.1002/jbio.200900070>
20. A. Mayevsky, R. Walden, E. Pewzner, A. Deutsch, E. Heldenberg, J. Lavee, S. Tager, E. Kachel, E. Rananani, S. Preisman, V. Glauber, and E. Segal, *J. Biomed. Opt.* **16**, 067004 (2011).  
<https://doi.org/10.1117/1.3585674>
21. D. J. Evers, R. Nachabe, D. Hompes, F. van Coevorden, G. W. Lucassen, B. H. W. Hendriks, M. L. van Velthuysen, J. Wesseling, and T. J. M. Ruers, *Eur. J. Surg. Oncol.* **39**, 68 (2013).  
<https://doi.org/10.1016/j.ejso.2012.08.005>
22. J. W. Spliethoff, W. Prevoo, M. A. J. Meier, J. de Jong, H. M. Klomp, D. J. Evers, H. J. C. M. Sterenberg, G. W. Lucassen, B. H. W. Hendriks, and T. J. M. Ruers, *Clin. Cancer Res.* **22**, 357 (2016).  
<https://doi.org/10.1158/1078-0432.CCR-15-0807>
23. E. Tanis, D. J. Evers, J. W. Spliethoff, V. V. Pully, K. Kuhlmann, F. van Coevorden, B. H. W. Hendriks, J. Sanders, W. Prevoo, and T. J. M. Ruers, *Lasers Surg. Med.* **48**, 820 (2016).  
<https://doi.org/10.1002/lsm.22581>
24. K. Kandurova, E. Potapova, V. Shupletsov, I. Kozlov, E. Seryogina, V. Dremin, E. Zherebtsov, A. Alekseyev, A. Mamoshin, and A. Dunaev, *Proc. SPIE* **11079**, 110791C (2019).  
<https://doi.org/10.1117/12.2526747>
25. A. C. Croce and G. Bottiroli, *Eur. J. Histochem.* **58**, 320 (2014).  
<https://doi.org/10.4081/ejh.2014.2461>
26. I. E. Rafailov, V. V. Dremin, K. S. Litvinova, A. V. Dunaev, S. G. Sokolovski, and E. U. Rafailov, *J. Biomed. Opt.* **21**, 025006 (2016).  
<https://doi.org/10.1117/1.JBO.21.2.025006>
27. K. Harris, D. J. Rohrbach, K. Attwood, J. Qiu, and U. Sunar, *J. Thorac. Dis.* **9**, 1386 (2017).  
<https://doi.org/10.21037/jtd.2017.03.113>
28. F. Braun, R. Schalk, M. Nachtmann, A. Hien, R. Frank, T. Beuermann, F. J. Methner, B. Kranzlin, M. Radle, and N. Gretz, *Meas. Sci. Technol.* **30**, 104001 (2019).  
<https://doi.org/10.1088/1361-6501/ab24a1>
29. M. C. Mathieu, A. Toullec, C. Benoit, R. Berry, P. Validire, P. Beaumel, Y. Vincent, P. Maroun, P. Vielh, and L. Alchab, *Eur. Radiol.* **28**, 2507 (2018).  
<https://doi.org/10.1007/s00330-017-5228-7>
30. J. W. Spliethoff, D. J. Evers, J. E. Jaspers, B. H. W. Hendriks, S. Rottenberg, and T. J. M. Ruers, *Transl. Oncol.* **7** (2) (2014).  
<https://doi.org/10.1016/j.tranon.2014.02.009>
31. T. Vo-Dinh, *Biomedical Photonics Handbook: Biomedical Diagnostics* (CRC, Boca Raton, FL, 2014).
32. A. Mayevsky and G. G. Rogatsky, *Am. J. Physiol. Physiol.* **292**, C615 (2007).  
<https://doi.org/10.1152/ajpcell.00249.2006>
33. G. Papayan, N. Petrishchev, and M. Galagudza, *Photodiagn. Photodyn. Ther.* **11**, 400 (2014).  
<https://doi.org/10.1016/j.pdpdt.2014.05.003>
34. M. M. Lukina, M. V. Shirmanova, T. F. Sergeeva, and E. V. Zagainova, *Sovrem. Tekhnol. Med.* **8**, 113 (2016).  
<https://doi.org/10.17691/stm2016.8.4.16>
35. A. A. Heikal, *Biomark. Med.* **4**, 241 (2010).  
<https://doi.org/10.2217/bmm.10.1>
36. K. Koenig and H. Schneckenburger, *J. Fluoresc.* **4**, 17 (1994).  
<https://doi.org/10.1007/BF01876650>
37. D. Wang, Y. Chen, and J. T. C. Liu, *Biomed. Opt. Express* **3**, 3153 (2012).  
<https://doi.org/10.1364/BOE.3.003153>
38. D. A. Loginova, E. A. Sergeeva, A. D. Krainov, P. D. Agrba, and M. Y. Kirillin, *Quantum Electron.* **46**, 528 (2016).  
<https://doi.org/10.1070/QEL16133>
39. E. V. Potapova, V. V. Dremin, E. A. Zherebtsov, K. V. Podmaster'ev, and A. V. Dunaev, *Fundam. Prikl. Probl. Tekh. Tekhnol.* **331**, 105 (2018).
40. P. R. Angelova and A. Y. Abramov, *FEBS Lett.* **592**, 692 (2018).  
<https://doi.org/10.1002/1873-3468.12964>
41. K. A. Foster, C. J. Beaver, and D. A. Turner, *Neuroscience* **132**, 645 (2005).  
<https://doi.org/10.1016/j.neuroscience.2005.01.040>
42. E. Zherebtsov, P. Angelova, S. Sokolovski, A. Abramov, and E. Rafailov, *Proc. SPIE* **10685**, 106854E (2018).  
<https://doi.org/10.1117/12.2307552>
43. Y. J. Kim, S. Mizushima, and H. Tokuda, *J. Biochem.* **109**, 616 (1991).  
<https://doi.org/10.1093/oxfordjournals.jbchem.a123429>
44. E. Takahashi, H. Endoh, M. Ishikawa, M. Kishi, and K. Doi, in *Oxygen Transport to Tissue XXIV* (Springer, Berlin, 2003), p. 565.  
[https://doi.org/10.1007/978-1-4615-0075-9\\_54](https://doi.org/10.1007/978-1-4615-0075-9_54)
45. K. Drozdowicz-Tomsia, A. G. Anwer, M. A. Cahill, K. N. Madlum, A. M. Maki, M. S. Baker, and E. M. Goldys, *J. Biomed. Opt.* **19**, 86016 (2014).  
<https://doi.org/10.1117/1.JBO.19.8.086016>
46. F. Bartolomé and A. Y. Abramov, *Methods Mol. Biol.* **1264**, 263 (2015).  
[https://doi.org/10.1007/978-1-4939-2257-4\\_23](https://doi.org/10.1007/978-1-4939-2257-4_23)
47. V. Weissig and M. Edeas, *Mitochondrial Medicine* (Humana, New York, 2015), Vol. 1.  
<https://doi.org/10.1007/978-1-4939-2257-4>
48. S. Mottin, P. Laporte, and R. Cespuglio, *Neurochem.* **84**, 633 (2003).  
<https://doi.org/10.1046/j.1471-4159.2003.01508.x>
49. V. Dremin, E. Potapova, E. Zherebtsov, I. Kozlov, E. Seryogina, K. Kandurova, A. Alekseyev, G. Piavchenko, S. Kuznetsov, A. Mamoshin, and A. Dunaev, *Proc. SPIE* **108770**, 108770K (2019).  
<https://doi.org/10.1117/12.2509255>
50. J. R. Lakowicz, *Principles of Fluorescence Spectroscopy* (Springer Science, New York, 2013).
51. Int. Commission on Non-Ionizing Radiation Protect., *Health Phys.* **87**, 171 (2004).  
<https://doi.org/10.1097/00004032-200408000-00006>
52. V. V. Dremin, E. A. Zherebtsov, V. V. Sidorov, A. I. Krupatkin, I. N. Makovik, A. I. Zherebtsova, E. V. Zharkikh, E. V. Potapova, A. V. Dunaev, A. A. Doronin, A. V. Bykov, I. E. Rafailov, K. S. Litvinova, S. G. Sokolovski, and E. U. Rafailov, *J. Biomed. Opt.* **22**,

- 085003 (2017).  
<https://doi.org/10.1117/1.JBO.22.8.085003>
53. V. Plakunov and Yu. Nikolaev, *Principles of Dynamic Biochemistry* (Logos, Moscow, 2017) [in Russian].
54. F. Sivandzade, A. Bhalarao, and L. Cucullo, *Bio-protocol*, **9**, e3128 (2019).  
<https://doi.org/10.21769/BioProtoc.3128>
55. G. Vargas, K. F. Chan, S. L. Thomsen, and A. J. Welch, *Lasers Surg. Med.* **29**, 213 (2001).  
<https://doi.org/10.1002/lsm.1110>
56. A. K. Bui, R. A. McClure, J. Chang, C. Stoianovici, J. Hirshburg, A. T. Yeh, and B. Choi, *Lasers Surg. Med.* **41**, 142 (2009).  
<https://doi.org/10.1002/lsm.20742>
57. K. Capriotti and J. A. Capriotti, *J. Clin. Aesthet. Dermatol.* **5**, 24 (2012).
58. K. Marren, *Phys. Sportsmed.* **39**, 75 (2011).  
<https://doi.org/10.3810/psm.2011.09.1923>
59. H. R. Pelzel, C. L. Schlamp, M. Waclawski, M. K. Shaw, and R. W. Nickells, *Invest. Ophthalmol. Vis. Sci.* **53**, 1428 (2012).  
<https://doi.org/10.1167/iovs.11-8872>
60. J. C. Rojas, J. A. Saavedra, and F. Gonzalez-Lima, *Brain Res.* **1215**, 208 (2008).  
<https://doi.org/10.1016/j.brainres.2008.04.001>
61. J. L. Hanslick, K. Lau, K. K. Noguchi, J. W. Olney, C. F. Zorumski, S. Mennerick, and N. B. Farber, *Neurobiol. Dis.* **34**, 1 (2009).  
<https://doi.org/10.1016/j.nbd.2008.11.006>
62. Z. W. Yu and P. J. Quinn, *Biosci. Rep.* **14**, 259 (1994).  
<https://doi.org/10.1007/BF01199051>
63. J. Galvao, B. Davis, M. Tilley, E. Normando, M. R. Duchon, and M. F. Cordeiro, *FASEB J.* **28**, 1317 (2014).  
<https://doi.org/10.1096/fj.13-235440>
64. N. D. Kirkpatrick, C. Zou, M. A. Brewer, W. R. Brands, R. A. Drezek, and U. Utzinger, *Photochem. Photobiol.* **81**, 125 (2005).
65. H. V. Danylovyh, *Ukr. Biochem. J.* **88**, 31 (2016).  
<https://doi.org/10.15407/ubj88.01.031>

*Translated by O. Zhukova*